Fiber transmission demonstrations in vector mode space division multiplexing

Leslie A. Rusch, Sophie LaRochelle

Springer, Frontiers of Optoelectronics, (Volume 11, Issue 2) (2018)

Doi: 10.1007/s12200-018-0812-2

https://link.springer.com/article/10.1007/s12200-018-0812-2

RESEARCH ARTICLE

Fiber transmission demonstrations in vector mode space division multiplexing

Leslie RUSCH (✉) and Sophie LAROCHELLE

Centre for Optics, Photonics and Lasers, ECE Dept., Université Laval, Quebec, G1V 0A6, CANADA

Abstract Much attention has been focused on the use of scalar modes for spatial division multiplexing (SDM). Alternative vector mode bases offer another solution set for SDM, expanding the available trade-offs in system performance and complexity. We present two types of ring core fiber conceived and designed to explore SDM with fibers exhibiting low interactions between supported modes. We review demonstrations of fiber data transmission for two separate vector mode bases: one for orbital angular momentum (OAM) modes and one for linearly polarized vector (LPV) modes. The OAM mode demonstrations include short transmissions using commercially available transceivers, as well as kilometer length transmission at extended data rates. The LPV demonstrations span kilometer length transmissions at high data rate with coherent detection, as well as a radio over fiber experiment with direct detection of narrowband signals.

Keywords space division multiplexing (SDM), few-mode fiber (FMF), orbital angular momentum (OAM), linearly polarized vector (LPV) modes, ring core fiber (RCF), polarization maintaining fiber

1 Introduction

Space division multiplexing (SDM) is being investigated to extend the carrying capacity of optical fiber, while continuing to drive down the cost per bit [1]. Promising research is underway to develop integrated components (running the gamut from couplers to add-drop multiplexers and switches) [2] to allow the cost-effective scaling of capacity. We focus on the development of optical fibers supporting multiple modes to push our understanding of the capabilities of SDM. Much of the activity in SDM research focuses on the use of scalar linearly polarized (LP) modes. In this paper, we explore the use of vector, rather than scalar, modes for SDM.

LP modes, studied for decades, are the solution of Maxwell's equation under the weakly guiding approximation where the difference between the index of refraction of the cladding and the core is very small. Such modes have significant interactions during propagation in recently developed few mode fibers (FMF) for SDM. A popular solution to overcome these interactions is the use of multiple input multiple output (MIMO) processing at reception [3]. The use of MIMO techniques relaxes requirements on all components in the SDM transmission link, as they can tolerate arbitrary coupling between modes, as long as mode dependent loss remains low [4].

The use of MIMO processing reduces system flexibility in some areas. For instance, we must capture all modes simultaneously and in synchrony. The receiver must process all modes in order to recover a single mode. In a mesh network, the use of SDM with MIMO would require that we route all modes on a given wavelength together. This increases the complexity of routers and limits the granularity of network routing, diminishing achievable network capacity. For shorter reach systems, MIMO processing makes up a significant share of overall receiver complexity and power consumption [5].

To offer an alternate set of system trade-offs, we can avoid the use of MIMO processing. To achieve this, we can design fibers and components that maintain the separation of modes and limit crosstalk [6-9]. While these systems may initially offer more limited reach (interactions will tend to increase with distance covered and components traversed), this is offset by the advantages of reduced receiver

E-mail: leslie.rusch@gel.ulaval.ca

complexity and eased network routing.

In section 2 we discuss the design of fibers for low cross-talk SDM transmissions. We introduce ring core fiber designs that offer two types of vector mode bases: one for orbital angular momentum (OAM) modes and the other for linearly polarized vector (LPV) modes. In section 3 we describe transmission experiments performed on OAM fibers. The demonstrations with commercial transceivers examine both a 10 Gb/s on-off keyed transmission with direct detection and a 100 Gb/s dual polarization QPSK transmission. Higher baud rate transmission at greater distance are achieved in our laboratory. No optical signal processing or tuning is required, and only two by two MIMO for polarization demultiplexing is required. In section 4 we describe transmission experiments performed on an elliptical ring core fiber supporting LPV modes. The first demonstration confirms the polarization maintaining property of these fibers and is free of optical or electronic processing to separate out individual transmissions. There is no MIMO processing. In addition to reporting wideband digital transmissions with coherent detection, we also examine narrowband radio over fiber transmissions with direct detection.

2 Ring core fiber designs

Standard telecommunication optical fibers are characterized by a step index profile with a small refractive index difference between the core and cladding materials. Under this so-called weakly guiding approximation, the cylindrical optical waveguide supports ensembles of vector eigenmodes that are nearly degenerate. These modes are grouped into scalar modes called linearly polarized modes and are labeled $LP_{\nu m}$, with index ν referring to the azimuthal symmetry and m to the radial dependence of the mode field. It is thus expected that the rotationally symmetric LP_{0m} modes will have two degenerate orthogonal polarization states. When $\nu>0$, $LP_{\nu m}$ mode groups are further composed of two degenerate spatial modes, each with two orthogonal polarization states, for a total of four degenerate modes. To reduce MIMO requirements, the optical fiber waveguide must be designed to increase the effective index separation between the true fiber eigenmodes, i.e., the vector modes. This propagation constant mismatch is a key factor in suppressing intra-mode coupling during propagation [10].

With respect to the effective index of the scalar mode, the effective index of a vector mode can be estimated using a first-order perturbative analysis [7]. Calculations show that the effective index difference will depend on the presence of a large refractive index gradient that overlaps with radial mode field component and large mode field variations. Ring core fibers with important refractive index steps therefore favor the separation of the effective indices between the fiber vector modes. Considering the first high order mode, LP_{11}, our goal is to introduce an effective index difference, δn_{eff}, of at least 1×10^{-4} between the TE_{01}, HE_{21} and TM_{01} modes; or in the case of the higher order mode groups, $LP_{\nu1}$ with $\nu>1$, between the $EH_{(\nu-1),1}$ and $HE_{(\nu+1),1}$ modes. The use of the ring core profile achieves this effective index separation, but some degeneracy remains between the EH^{odd}/EH^{even} and between the HE^{odd}/HE^{even} mode pairs. These mode pairs, become the basis of the OAM modes. Each OAM mode therefore has two degenerate orthogonal circular polarization states with opposite topological charge.

Elliptical core waveguides are widely used to split the degeneracy of polarization states, reduce mode coupling and offer polarization maintaining properties to the optical fiber. However, few demonstrations of few mode polarization maintaining fibers have been achieved due to the difficulty to reach sufficient effective index separation while keeping higher order modes above cut-off [11].

In this work, we present two optical fibers with ring cores for transmission over vector modes, as represented in Fig. 1. The core is germanium-doped silica with refractive index n_1, while the inner and outer cladding are made of silica with refractive index n_2. The first fiber (Fig. 1a) is a circularly symmetric ring core fiber (RCF) for OAM mode transmission and the second fiber (Fig. 1b) is an elliptical ring core fiber (ERCF) for transmission over non-degenerate LPV modes.

2.1 Ring core fiber (RCF) design for OAM

OAM modes in optical fibers are characterized by an annular intensity profile (m=1), an azimuthally varying phase, i.e., $exp(\pm il\phi)$ where $\pm l$ is the topological charge, and circular polarization. When designing ring core fibers for OAM mode transmissions, the thickness of the ring waveguide is controlled to insure that modes with m>1 are cut-off. In turn, the ring diameter allows the control of the number of OAM modes. In [6], we examined the cut-off conditions and parameter optimization space of ring core fibers for OAM modes. For the work presented in this paper, we chose an optical fiber supporting two OAM modes

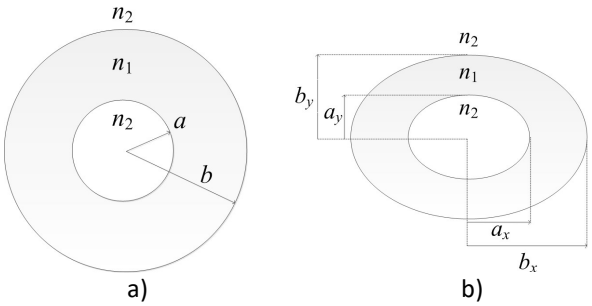

Fig. 1 Geometry of a) a ring core fiber and b) an elliptical ring core fiber.

(OAM±1). This RCF fiber design is labeled Fiber#2 in [6]. The designed inner and outer fiber radius were a=0.97 μm and b=2.78 μm for a ratio of $\rho=a/b$=0.35. The designed index step was n_1-n_2=0.03 resulting in a normalized frequency, here defined using the outer radius, $V=(2\pi b/\lambda)(n_1^2-n_2^2)^{1/2}$=3.3 at a wavelength of 1.55 μm. It should be noted that, although the design meets the $\delta n_{eff}>1\times10^{-4}$ criteria, it does not correspond to the optimum design for which $\delta n_{eff}>1.9\times10^{-4}$. This RCF design with $\delta n_{eff}>1.5\times10^{-4}$ was rather selected to make a fiber preform compatible with the fabrication of subsequent fibers supporting a larger number of OAM modes.

2.2 Elliptical ring core fiber (ERCF) design for LPV

The second fiber design is an elliptical ring core fiber (ERCF), as represented in Fig. 1b. This fiber is characterized by an ellipticity defined as $\eta=b_x/b_y=a_x/a_y$. Starting with a ring core fiber design that splits the {TE_{01}, HE_{21}, TM_{01}} modes, as well as the {EH_{11}, HE_{31}} modes, the ellipticity of the ring core fiber is increased to further lift the degeneracy of the HE_{21}, EH_{11}, HE_{31} odd and even mode pairs. The resulting modal basis is composed of vector eigenmodes with linear polarization and, for this reason, are designated as linearly polarized vector (LPV) modes [12]. The design target for this fiber was to achieve a birefringence $\delta n_{eff}>1\times10^{-4}$ for the first eight higher order modes. The fundamental mode (HE_{11} or LP_{01}) remains degenerate by design. The fiber has core radii along the long axis of a_x=3.4 μm and b_x=5.1 μm, which corresponds to a ratio ρ=0.67, and an ellipticity η=1.4. The index step was the same as the RCF, *i.e.,* n_1-n_2=0.03, resulting in a normalized frequency V=5.2, which is now defined using the average value of the outer radius, of $V=(\pi(b_x+b_y)/\lambda)(n_1^2-n_2^2)^{1/2}$. This design met the goal of four spatial modes with modal birefringence of $\delta n_{eff}>1.2\times10^{-4}$ resulting in eight LPV modes [12]. This birefringence grants polarization maintaining properties to the fiber and allows data transmission over the fiber LPV modes without MIMO over short distances, i.e., a few kilometers. The calculated effective index difference between spatial modes was larger than 1×10^{-3}.

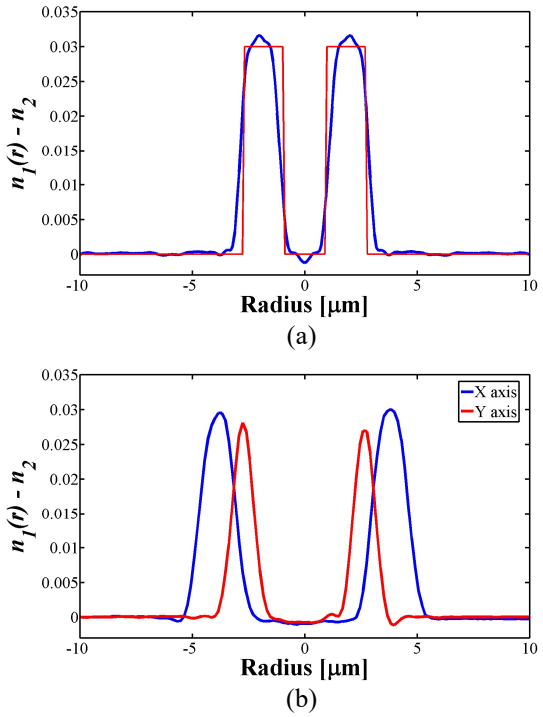

Fig. 2 Refractive index profile of a) ring core fiber showing the design (red) and the measured profile (blue), and b) an elliptical ring core fiber showing the measured profile along the two axis of the ellipse.

A first order perturbation analysis shows that large effective index separation between vector modes require large effective index gradient collocated with large transverse field and field divergence [7]. In multimode fibers, it is difficult to achieve large birefringence of the fundamental mode since this mode becomes more confined in the core. In our design, we successfully lifted the degeneracy of higher modes by introducing a fiber central region of higher index, but the resulting fundamental mode area was severely reduced. Consequently, we accept that the fundamental mode would not be polarization maintaining. Subsequently, introducing a central air hole has been proposed to lift this degeneracy [13]; to our knowledge, no experimental demonstration has yet been reported.

2.3 Fiber fabrication and characterization

The optical fiber preforms were fabricated at the COPL, Université Laval, using modified chemical vapor deposition (MCVD). In the case of the ERCF, the preform was polished on two sides before being rounded and drawn into an optical fiber. Fiber drawing is also done in-house. The measured refractive index profiles of the RCF is shown in Fig. 2a. The measurement was performed at 657.6 nm with an EXFO NR-9200. Figure 2b shows the refractive index profile of the ERCF done at 633 nm (Interfiber Analysis).

The effective index separation between modes was measured by writing fiber Bragg gratings (FBGs) in the optical fibers [14]. The fibers were first deuterium loaded before FBGs were photoinduced by phase mask scanning using a 244 nm UV laser. In the reflection spectrum, the difference in the Bragg wavelengths of each modes is directly related to the effective index difference. The method can therefore be used to measure the separation of the spatial modes, as well as the modal birefringence. Figure 3 shows the FBG measurement for both fibers. The wavelength, λ, is referenced to the Bragg wavelength of the fundamental mode, λ_{B0}, in both cases.

In RCF, the Bragg peaks associated to the {TE_{01}, HE_{21}, TM_{01}} modes are clearly visible between λ-λ_{B0}=-8 to -9

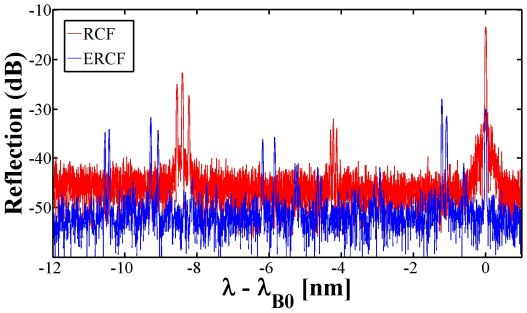

Fig. 3 Reflection spectrum of fiber Bragg gratings written in the ring core fiber (RCF, red) and the elliptical ring core fiber (ERCF, blue).

nm, while peaks near λ-λ_{B0}=-4 nm corresponds to cross-coupling of the higher order modes with the fundamental mode. The measured wavelength shift between the Bragg peaks of the vector modes, shows that the minimum δn_{eff} occurred between the TM_{01} and HE_{21} modes and was $\delta n_{eff}=1.4\times10^{-4}$ in the fabricated fiber (compared to the calculated value of 1.5×10^{-4}) [6].

The FBG reflection spectrum of the ERCF fiber clearly shows the four spatial modes as four double peaks. The splitting of these peaks is related to δn_{eff} between the two polarization modes. In this case, the minimum δn_{eff} occurred between the two polarization states of the LPV_{21b} mode ($\delta n_{eff}=1\times10^{-4}$,). Although this mode was observed after short fiber lengths of a few meters, its high loss made it unusable for long distance transmission. For the remaining six LPV modes used for transmission, the minimum mode separation was $\delta n_{eff}=1.25\times10^{-4}$ [9].

The fabricated RCF fiber provides four channels for data transmission with 2×2 MIMO: the two orthogonal polarization states of the fundamental mode (also called OAM0), and the two degenerate OAM+1 and OAM-1 modes with orthogonal circular polarization states. This fiber also supports TE_{01} and TM_{01} modes that form unstable OAM modes. Theses modes are not used for transmission but their presence can act as a cross-talk path between the propagating OAM+1 and OAM-1 modes [15]. Due to its modal birefringence, the fabricated ERCF has six polarization maintaining modes that are above cut-off {LPV^{y}_{11a}, LPV^{x}_{11a}, LPV^{x}_{11b}, LPV^{y}_{11b}, and LPV^{x}_{21a}}. In addition, the fundamental mode with the two degenerate orthogonal polarization states is also present, but is not used to carry data as our goal with this fiber is to achieve MIMO less transmission.

3 Transmission over OAM RCF

As discussed in [16], the OAM modes will mix in polarization, but each mode should maintain good orthogonality if the effective refractive indices are sufficiently spread per the discussion in the previous section. Our goal then is to accept 2×2 MIMO for polarization recovery, but to eschew the use of MIMO to separate out modal interactions. We performed several series of transmission experiments with our OAM ring core fiber to validate this concept. The first experiment was at limited distances and used commercial transceivers. We ran the second series at 1.1 km lengths and used laboratory test equipment with off-line data processing.

3.1 Bulk component mux and demux

All experimentation with the OAM RCF fiber used the multiplexer (MUX) and demultiplexer (DEMUX) described in Fig. 4. Programmable spatial light modulators (SLMs) based on liquid crystal technology provide a convenient, flexible method of generating OAM modes (MUX) and converting OAM modes to the fundamental mode (DEMUX). However, the SLMs are polarization sensitive, making their use somewhat cumbersome for a polarization-multiplexed system. The polarization beam splitters (PBS), half wave plates (HWP) and quarter wave plates (QWP) allowed us to manipulate the polarization and convert the vertically polarized SLM1 output in the MUX to the circular polarization (left or right) required for good fiber propagation of OAM modes in the ring core fiber. Spiral phase patterns were programmed on SLM1 for OAM generation.

At the DEMUX end, there are two output ports. One path is simply coupled to a single mode fiber (SMF). Given the annular intensity profile of the OAM modes, the SMF acts as a mode stripper, so that only the fundament mode is delivered to the receiver on this path.

The second port of the DEMUX uses the SLM programmed with blazed forked gratings to convert the incoming OAM modes to the fundamental mode. Two paths are provided to the SLM, so that the two circular polarizations can be captured via two projections onto the linear polarization supported by the SLM. SLM2 shifts to an OAM mode the data originally transmitted on the fundamental mode; by the same operation, SLM2 shifts data on the OAM mode in the fiber to the fundamental mode. Once the two paths have the OAM channel converted to fundamental, the two polarization contributions are combined, and coupled to SMF. The data originally transmitted on the fundamental mode (now on OAM) is rejected by the SMF.

3.2 Commercial transceivers at short distances

As reported in [16], short lengths (first 3.75 m, then 100 m) of OAM RCF fiber were used to transmit heterogeneous traffic on two separate modes. The fundamental mode was used to carry on-off keying data at 10 Gb/s with direct detection. The OAM modes were used to carry 100 Gb/s QPSK data using polarization multiplexing and exploiting coherent detection. Commercial receivers from

Huawei were used for both channels and no special software or optical signal processing was required.

At the shorter length, we observed error free transmission (bit error below 1e-12) over a long observation window. At the longer length, the pre-forward error correction (FEC) was degraded, but bit error rate remained well within tolerable levels. The greatest source of impairments was the free space coupling, as the experimental environment was susceptible to vibrations.

These experiments were the first demonstration of the compatibility of OAM transmissions with commercial equipment. Our fibers were capable of maintaining modal separation, effectively creating two independent channels with reliable communications links. We confirmed that standard 2×2 MIMO for polarization was sufficient for good reception in the OAM channel despite the presence of OOK data on the fundamental mode.

3.3 Transmission at 1.4 km

We performed extensive experimentation with a 1.4 km length of OAM RCF fiber, examining both transmission performance [17] and assessing the impact of modal interactions on that performance [15]. The objective of the transmission experiments was to probe the achievable bit rates given the significant crosstalk and our desire to avoid the use of extensive multiple input, multiple output processing. As in the experiments of the previous section, the two output ports have data processed independently without any synchronization or joint processing.

We were careful during the coupling process to balance the crosstalk levels seen by the fundamental and OAM±1 modes in either polarization. Crosstalk levels between any pair of modes was virtually identical, at -13.5 dB, and cumulative crosstalk was -10.5 dB. The additional power penalty was a few dB up to crosstalk of -9 dB, but grew steeply after that. Several components in the free space alignment stage responded to temperature variations and air movement, leading to crosstalk increases. We assured good isolation from these effects by the simple expedient of boxing the translation stage.

Transmission was successful at baud rates from 16 Gbaud to 32 Gbaud [17]. The OAM modes suffered the most impairment, although the measured crosstalk levels were similar to that of the fundamental mode. The OAM modes approached the 3.8×10^{-3} forward error correction (FEC) threshold at 32 Gbaud operation. When sending one mode at a time, the OAM modes also experienced somewhat diminished performance compared to the fundamental.

Given these observations, we embarked on a closer examination in [15] of the source of the differentiated performance in the face of similar crosstalk. We were able to identify the influence of parasitic vector modes. The fiber supports TE_{01} and TM_{01}, but they not used for communications. As they are not used, there is no visibility at the receiver into these modes. We refer to these modes as parasitic as they can siphon off energy from the desired modes, and act as a conduit for leakage between modes.

Our channel characterization led us to identify pulse broadening in the OAM modes that was not present on the fundamental mode. Time of flight experiments confirmed that the parasitic modes had propagation constants very similar to that of the OAM mode, but far from that of the fundamental mode. Despite the effective index separation between the parasitic modes and the OAM mode, there was energy exchange among them.

The parasitic modes lead to an increase in equalizer length for the 2×2 MIMO for OAM modes vis-à-vis the fundamental modes. This added complexity runs counter to goals in avoiding full MIMO processing. We note however, that the two parasitic modes are only present in proximity to OAM±1. When scaling to higher modes, this will lead to only one mode (OAM±1) with increased equalizer lengths. We expect the higher order modes to have perfor-

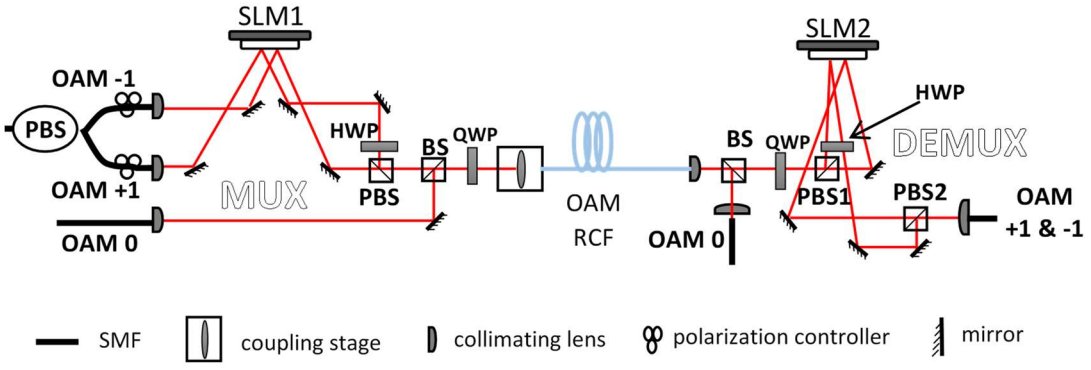

Fig. 4 Setup for transmission experiments. In experiments with commercial transceivers, OAM0 uses OOK transceiver with direct detection, while OAM±1 uses QPSK transceiver with coherent detection. In experiments with a real-time oscilloscope, QPSK with coherent detection is used on both OAM0 and OAM±1.

mance similar to that of the fundamental, i.e., without parasitic effects.

4 Transmission over LPV ERCF

We performed two series of transmission experiments with our ERCF supporting LPV modes. The fundamental modes had polarizations that coupled during transmission, so we did not exploit these modes, leaving them unused.

4.1 Bulk component mux and demux

Figure 5 gives the experimental setup for the LPV transmissions over ERCF. We perform the multiplexing and demultiplexing in bulk optics, as in the previous section. Further details on the setup are available in [9]. The six inputs are data modulated and decorrelated in time. The polarizations are set at launch to align with the fiber input orientation, hence the polarization controllers on the MUX stage. We make no effort at the receiver, neither in optics nor in electronics, to undo polarization rotation or mixing. The polarizer at the DEMUX stage simply selects one of two polarizations states before mode detection via SLM2.

4.2 Wideband transmission over 6 modes

We transmitted six independent channels of QPSK data over 0.9 km of LPV ERCF [9]. We applied a single stage detector in round-robin fashion to detect each channel in turn. We used the polarizer to select one of the orthogonal polarizations (X or Y), thus rejecting half of the channels. We next programmed the pattern on SLM2 to one of three settings: LPV_{11a}, LPV_{11b} or LPV_{21a}. In this way, each of the six channels could be detected with a single DEMUX stage.

The crosstalk we observed between any two data channels was never greater than -14 dB. The total crosstalk on a single mode from all other modes combined varied from -9 to -10.5 dB. These crosstalk levels allowed for transmission rates as high as 32 Gbaud while remaining under the FEC threshold. The bit error rate per channel was spread across 3.8×10^{-8} to 2×10^{-4} due to the unequal crosstalk levels. We demonstrated transmission of 179 Gb/s (allowing for the 7% FEC overhead) over a single elliptical core on one wavelength. Other demonstrations with OOK [18] were limited to throughput of 30 Gb/s as they could not exploit polarization independence in their elliptical core fiber.

We accomplished transmission with no polarization tracking or tweaking. The digital signal processing used no MIMO processing whatsoever. The coherent detector in this experiment had an input local oscillator whose polarization we aligned to the detected mode (selected by the polarizer). This allowed us to monitor only one IQ output, thus allowing the possibility of a less complex receiver. Alternately, we could have left the local oscillator without polarization alignment, and the two pairs of IQ outputs would then be combined before detection to achieve polarization diversity.

4.3 Narrowband transmission over 4 modes

The next series of experiments involved the transmission of narrowband radio over fiber signals. This type of signaling is typical for transport of front haul traffic between base stations and remote radio heads. The advent of pooled base band units will see great increase in front haul requirements, particularly as 5G services come on line.

The greater sensitivity of narrowband signals to inband crosstalk led us to multiplex only four channels in this experiment. The setup in Fig. 5 was modified accordingly. The upper branch (inputs 5 and 6) was eliminated and the

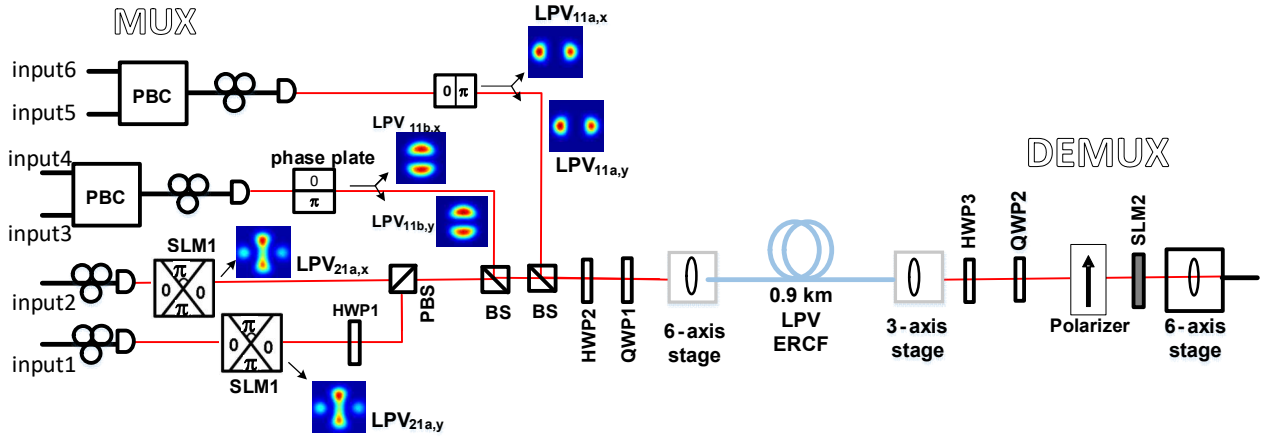

Fig. 5 Setup for transmission experiments with LPV modes. In wideband experiments, QPSK data is transmitted on all modes and coherent detection is used. In narrowband radio over fiber experiments, only four channels are populated: inputs 5 and 6 are unused and input 2 generates $LPV_{11a,x}$.

path for input 2 was modified to generate $LPV_{11a,x}$. Further details are available in [19].

We transmitted four independent channels of 16QAM data over 0.9 km o LPV ERCF [9]. Each channel was an orthogonal frequency division multiplexed (OFDM) signal occupying 480 MHz, for a total bit rate of 1.1 Gb/s per mode. We examined two RF carrier frequencies: 2.4 and 3.3 GHz. We used the single DEMUX stage, as in the previous section, to separate channels for direct detection.

The crosstalk we observed between any two data channels was never greater than -14 dB. The total crosstalk from all modes combined onto a single mode varied within one dB of -12 dB. Despite these significantly lower total crosstalk levels (due to using four rather than six modes), all four channels operated near the FEC threshold. Clearly, the OFDM signals are more sensitive to modal crosstalk, as might be expected when using a single tap equalizer. Equalizers in the wideband experiment had 11 taps.

5 Conclusion

We presented two types of fibers with low intermodal crosstalk. In both cases, our goal was to demonstrate the ability to multiplex spatially and incur only minimal MIMO requirements at the receiver. When using LPV modes in ERCF we were able to receive with no MIMO processing whatsoever, and no polarization tracking. When using OAM modes in RCF the MIMO requirements were limited to separation of polarizations, and could be achieved even when using commercial transceivers conceived for operation with SMF; no polarization tracking was required.

References

1. Richardson DJ, Fini JM, and Nelson LE, Space-division multiplexing in optical fibres. Nature Photonics, 2013, 7(5): 354-362.
2. Marom DM, Colbourne PD, D'Errico A, Fontaine NK, Ikuma Y, Proietti R, Zong L, Rivas-Moscoso JM, and Tomkos I, Survey of Photonic Switching Architectures and Technologies in Support of Spatially and Spectrally Flexible Optical Networking [Invited]. Journal of Optical Communications and Networking, 2017, 9(1): 1-26.
3. Fontaine NK, Ryf R, Chen H, Benitez AV, Guan B, Scott R, Ercan B, Yoo SJB, Grüner-Nielsen LE, Sun Y, Lingle R, Antonio-Lopez E, and Amezcua-Correa R. 30×30 MIMO Transmission over 15 Spatial Modes. In Optical Fiber Communication Conference Post Deadline Papers. Los Angeles, California: 2015. Th5C.1.
4. Huang B, Fontaine NK, Ryf R, Guan B, Leon-Saval SG, Shubochkin R, Sun Y, Lingle R, and Li G, All-fiber mode-group-selective photonic lantern using graded-index multimode fibers. Optics Express, 2015, 23(1): 224-234.
5. Arik SO, Askarov D, and Kahn JM. MIMO DSP Complexity in Mode-Division Multiplexing. In Optical Fiber Communication Conference. Los Angeles, California: 2015. Th1D.1.
6. Brunet C, Ung B, Wang L, Messaddeq Y, LaRochelle S, and Rusch LA, Design of a family of ring-core fibres for OAM transmission studies. Optics Express, 2015, 23(8): 10553-10563.
7. Ung B, Wang L, Vaity P, Jin C, Rusch LA, Messaddeq Y, and LaRochelle S, Few-mode fiber with inverse-parabolic graded-index profile for transmission of OAM-carrying modes. Optics Express, 2014.07.28, 22(15): 18044-18055.
8. Brunet C, Vaity P, Messaddeq Y, LaRochelle S, and Rusch LA, Design, fabrication and validation of an OAM fiber supporting 36 states. Optics Express, 2014, 22(21): 26117-26127.
9. Wang L, Nejad RM, Corsi A, Lin J, Messaddeq Y, Rusch LA, and LaRochelle S, Linearly polarized vector modes: enabling MIMO-free mode-division multiplexing. Optics Express, 2017, 25(10): 11736-11749.
10. Antonelli C, Mecozzi A, Shtaif M, and Winzer PJ, Random coupling between groups of degenerate fiber modes in mode multiplexed transmission. Opt Express, 2013, 21(8): 9484-90.
11. Liang J, Mo Q, Fu S, Tang M, Shum P, and Liu D, Design and fabrication of elliptical-core few-mode fiber for MIMO-less data transmission. Opt Lett, 2016, 41(13): 3058-61.
12. Wang L and LaRochelle S, Design of eight-mode polarization-maintaining few-mode fiber for multiple-input multiple-output-free spatial division multiplexing. Opt Lett, 2015, 40(24): 5846-9.
13. Zhao J, Tang M, Oh K, Feng Z, Zhao C, Liao R, Fu S, Shum PP, and Liu D, Polarization-maintaining few mode fiber composed of a central circular-hole and an elliptical-ring core. Photonics Research, 2017, 5(3): 261-266.
14. Wang L, Vaity P, Ung B, Messaddeq Y, Rusch LA, and LaRochelle S, Characterization of OAM fibers using fiber Bragg gratings. Opt Express, 2014, 22(13): 15653-61.
15. Nejad MR, Wang L, Lin J, LaRochelle S, and Rusch LA, The Impact of Modal Interactions on Receiver Complexity in OAM Fibers. Journal of Lightwave Technology, 2017, 35(21): 4692-4699.
16. Rusch LA, Rad MM, Allahverdyan K, Fazal I, and Bernier E, Carrying data on the orbital angular momentum of light. IEEE Communications Magazine, 2018, 56(2): 219 - 224.
17. Mirzaei Nejad R, Allahverdyan K, Amiralizadeh S,

Brunet C, LaRochelle S, and Rusch LA, Mode Division Multiplexing using Orbital Angular Momentum Modes over 1.4 km Ring Core Fiber. IEEE/OSA Journal of Lightwave Technology, 2016, 34(18): 4252-4258.

18. Parmigiani F, Jung Y, Grüner-Nielsen L, Geisler T, Petropoulos P, and Richardson DJ, Elliptical Core Few Mode Fibers for Multiple-Input Multiple Output-Free Space Division Multiplexing Transmission. IEEE Photonics Technology Letters, 2017, 29(21): 1764-1767.
19. Mirzaei Nejad R, Tavakoli F, Wang L, Guan X, LaRochelle S, and Rusch LA, *Four-Channel RoF Transmission over Polarization Maintaining Elliptical Ring Core Fiber* in *IEEE/OSA Optical Fiber Communications Conference (OFC 2018)*. 2018: San Diego. p. M4J.6.